Supplemental Materials

Change of crackling noise in granite by thermal damage: monitoring

nuclear waste deposits

Kainan Xie[1,6], Xiang Jiang[1,2,3*], Deyi Jiang[1], Yang Xiao[2], Shiwan Chen[4],

Karin A. Dahmen[5], Eduard Vives[6], Antoni Planes[6], Ekhard K.H. Salje [3,7]

[1] State Key Laboratory of Coal Mine Disaster Dynamics and Control, Chongqing

University, Chongqing 400044, P.R. China

[2] College of Civil Engineering, Chongqing University, Chongqing 400045, P.R.

China

[3] Department of Earth Sciences, University of Cambridge, Cambridge CB2 3EQ,

United Kingdom

[4] College of Resources and Environment Engineering, Guizhou University, Guiyang,

550025, P.R. China

[5] Department of Physics, University of Illinois at Urbana Champaign, Urbana, IL

61801, United States

[6] Departament de Física de la Matèria Condensada. Facultat de Física, Universitat de

Barcelona. Martí i Franquès, 1, 08028 Barcelona, Catalonia.

[7] State Key Laboratory for Mechanical Behaviours of Materials, Xi'an Jiao Tong

University, Xi'an 710049, P.R. China.

*Corresponding author: cqujiangxiang@163.com

BEISHAN AND THE GRANITE SAMPLE DESCRIPTION

The rock samples were collected from Beishan in the northwest of China (Supplemental figure1a). The study area is a low mountain, hilly terrain, generally 1600 ~ 1700m above sea level. The study area is a continental semi desert. The annual rainfall is 78.9mm and the annual evaporation capacity is near 3130.9mm, vegetation is sparse. All Beishan Granite (BsG) samples (Supplemental figure 1b.) were taken from one macroscopically homogeneous granite block. Subsequently, the sample preparation was applied following the International Society for Rock Mechanics (ISRM) testing guidelines (Fairhurst and Hudson 1999). The natural density of BsG is about 2.61 g/cm^2. The main mineral components of BsG are quartz (34.09%), feldspar (60.59%), and biotite (5.32%), as determined by X-ray diffraction (Supplemental figure 1d.). In the eastern part of the pluton, potassium/argon isotope dating showed an age of 259 Ma.

THE NMR EXPERIMENT EQUIPMENT AND PARAMETER SETTING

The NMR instrument (MacroMR12-150H-I) (Supplemental figure 2a) was supplied by Niuman Corporation (Shanghai, China), the centrifuge and high-pressure device were supplied by Huaxing Company (Jiangsu, China). Water was compressed into the samples using a simple pressure device (Supplemental figure 2b). The magnetic field of the NMR is 0.3T in X, Y, and Z directions with a gradient value of 1 T/m. The radio frequency (RF) lies in the range of 1–42 MHz with a control accuracy of 0.01 Hz. All the experiments are performed at the constant temperature of $32.0 \pm 0.02°C$. T_2 relaxation is measured using the Carr-Purcell-Meiboom-Gill (CPMG) pulse sequence. The NMR apparatus specific parameters are shown in Supplemental table 1. The CPMG echo train comprises a 90°pulse, followed by a train of 180° pulses. This pulse sequence eliminates de-phasing effects produced by local variations in the magnetic field and therefore measures the true T_2 of the sample. The signal decay is due to interactions with neighboring spins and surfaces. The CPMG pulse sequence takes only a few seconds to run, which makes it practical both in the laboratory and for well logging applications. The T_2 relaxation measurements were performed at 32.0°C. The parameter settings for the CPMG pulse sequence used for the BsG samples are summarized in Supplemental Table 2. The parameter settings for MRI are shown in Supplemental Table.3. The cross-section that is located in the middle of the column with 2mm in width.

In water-saturated rock samples, the T_2 curve related to a single pore is proportional to pore size (Al-Mahrooqi et al. 2003) where large pores have large T_2 values while small pores have small T_2 values (Li et al. 2008). The T_2 curve of NMR related to a single pore is proportional to pore size, for fluids within porous materials, three independent relaxation mechanisms occur: (1) bulk relaxation which is an intrinsic property of the fluid, (2) surface relaxation at the fluid-solid interface and (3) diffusion induced relaxation in a gradient field. The total relaxation can be expressed as (Toumelin et al. 2007; Yun et al. 2002)

$$(\frac{1}{T_2})_{total} = (\frac{1}{T_2})_S + (\frac{1}{T_2})_D + (\frac{1}{T_2})_B \tag{1}$$

The relaxation of water is mainly caused by the collision with the particle surface in water-saturated core, which mainly determined by surface relaxation, and its closely related to surface volume ratio of the pore (Kenyon et al. 1995; Kleinberg et al. 1994; Müller-Huber et al. 2016). The signal strength of MRI represents the density of ^{1}H which in a material. In detail, in our study the MRI can identify the rock and water because water has much more protons than the rock skeleton. As the cracks and pores are filled by water, we can capture the signals, which come from water to locate the cracks. The color bar in this paper provides a relative scale for the moisture content. In addition, T_2-weighted images used in our study emphasize the area where a high mobility proton is present (Dong et al. 2017; Hong et al. 2009).

THE AE EXPERIMENT EQUIPMENT AND PARAMETER SETTING

The AE signals were measured during compression by two piezoelectric sensors (NANO-30 Physical Acoustics Company) fixed to the sample's round surface by rubber bands. The sensors were acoustically coupled to the sample by a thin layer of grease. The acoustic signal was pre-amplified (40 dB) and transferred to the AE analysis system (DISP from the Physical Acoustics Company, see Supplemental figure 3). The threshold for detection was chosen as the threshold of an empty experiment (45 dB). The Peak Definition Time (PDT) was 35 µs, the Hit Definition Time (HDT) was 150 µs, and the Hit Lockout Time (HLT) was 300 µs. The PDT setting was chosen to ensure the correct identification of the signal peak for rise-time and peak amplitude measurements. The HDT setting was selected to ensure that each AE signal from the structure was reported once only. The HLT setting was selected to avoid spurious measurements during the signal decay and to increase data acquisition speed.

THE THERMAL DAMAGE AND FAILURE OBSERVATION

An inverted metallurgical microscope and a low-field NMR were used to investigate the thermal damage at the surface and in the core. Optical microscopic observations for BsG samples at various annealing temperatures are shown in Supplemental Figure.4. No micro cracks were observed below 300°C. Heating samples to 600°C and 700°C generates cracks inside quartz grains, related to the rapid thermal expansion near the α/β transition at T=573°C (Somerton 1992). This transition is independent of the grain size (Aufort et al. 2015) with elastic moduli decreasing near the transition point (Carpenter et al. 1998). The constant macroscopic linear thermal expansion of granite holds between 200°C and 500°C, and increases on further heating (Lin 2002) Simultaneously, cracks are generated with large inter-grain stresses from differential thermal expansion at grain boundaries.

REFERENCES

Al-Mahrooqi, S.H., Grattoni, C.A., Moss, A.K., Jing, X.D. (2003) An investigation of the effect of wettability on NMR characteristics of sandstone rock and fluid systems. Journal of Petroleum Science and Engineering, 39, 389-398.

Aufort, J., Aktas, O., Carpenter, M.A., Salje, E.K.H. (2015) Effect of pores and grain size on the elastic and piezoelectric properties of quartz-based materials, American Mineralogist, 100, 1165-1171.

Carpenter, M.A., Salje, E.K.H., Graemebarber, A., Dove, M.T., Knight, K.S. (1998) Calibration of excess thermodynamic properties and elastic constant variations associated with the α ↔ β phase transition in quartz, American Mineralogist, 83, 2-22.

Dong, X., Li, Y., Li, Y., Song, L., Cheng, S., Li, D. (2017) Combination of NMR and MRI Techniques for Non-invasive Assessment of Sea Cucumber (Stichopus japonicas) Tenderization During Low-Temperature Heating Process. Food Analytical Methods, 10, 2207–2216.

Fairhurst, C.E., and Hudson, J.A. (1999) International society for rock mechanics commission on testing methods. International Journal of Rock Mechanics and Mining Sciences, 36, 279–289.

Hong, Y.S., Jeehyun, C., Nari, K., Chulhyun, L., Chaejoon, C., KwanSoo H. (2009)

Artifacts in the measurement of water distribution in soybeans using MR imaging. Food Chemistry, 112, 267-272.

Kenyon, W.E., Takezaki, H., Straley, C., Sen, P.N., Herron, M., Matteson, A. (1995) A laboratory study of nuclear magnetic resonance relaxation and its relation to depositional texture and petrophysical properties: carbonate Thamama Group, Mubarraz Field, Abu Dhabi. Middle East Oil Show Proc.

Kleinberg, R.L., Kenyon, W.E., Mitra, P.P. (1994) Mechanism of NMR Relaxation of Fluids in Rock, Journal of Magnetic Resonance, 108, 206-214.

Li, H.B., Zhu, J.Y., Guo, H.K. (2008) Methods for calculating pore radius distribution in rock from NMR T_2 spectra, Chinese Journal of Magnetic Resonance, 25, 273-280.

Lin, W. (2002) Permanent strain of thermal expansion and thermally induced microcracking in Inada granite, Journal of Geophysical Research, 107, 3-16.

Müller-Huber, E., Schön, J., Börner, F. (2016) Pore space characterization in carbonate rocks-Approach to combine nuclear magnetic resonance and elastic wave velocity measurements. Journal of Applied Geophysics, 127, 68-81.

Somerton, W.H. (1992) Thermal Properties and Temperature Related Behaviour of Rock/Fluid Systems. Journal of Volcanology and Geothermal Research, 56, 171-172.

Toumelin, E., Torres-Verdin, C., Sun, B., Dunn, K.J. (2007) Random-walk technique for simulating NMR measurements and 2D NMR maps of porous media with

relaxing and permeable boundaries. Journal of Magnetic Resonance, 188, 83-96.

Yun, H., Zhao, W., Zhou, C. (2002) Researching Rock Pore Structure with T_2 Distribution, Well Logging Technology, 26, 18-21.

**Supplemental Table S1.** The parameters of NMR test system.

Parameters	Value
Magnetic field intensity	0.3T
Pulse frequency range	1MHz∼42MHz
Pole diameter	374mm;
Pole gap	110mm
Magnetic field uniformity	25ppm
Maximum sampling bandwidth	2000KHz
Magnet temperature	32℃

**Supplemental Table S2.** Parameter settings for NMR CPMG pulse sequence

| Parameters	Value
Signal Frequency	12MHz
Frequency Offset	681668.8Hz
scanning number	64
Recycle delay	0.2ms
Number of echos	15000
Radio-frequency pulse width for 90º	15.6μs
Radio-frequency pulse width for 180º	31.2μs
Waiting time	1.0s
Echo time	0.19ms

Supplemental Table S3. Parameter settings for MRI

| Parameters	Value
Frequency Offset	682626 Hz
scanning number	16
Flip Angle	90 $^{\circ}$
Refoc Flip Angle	180 $^{\circ}$
Echo time	6 ms
Repetition time	1000 ms
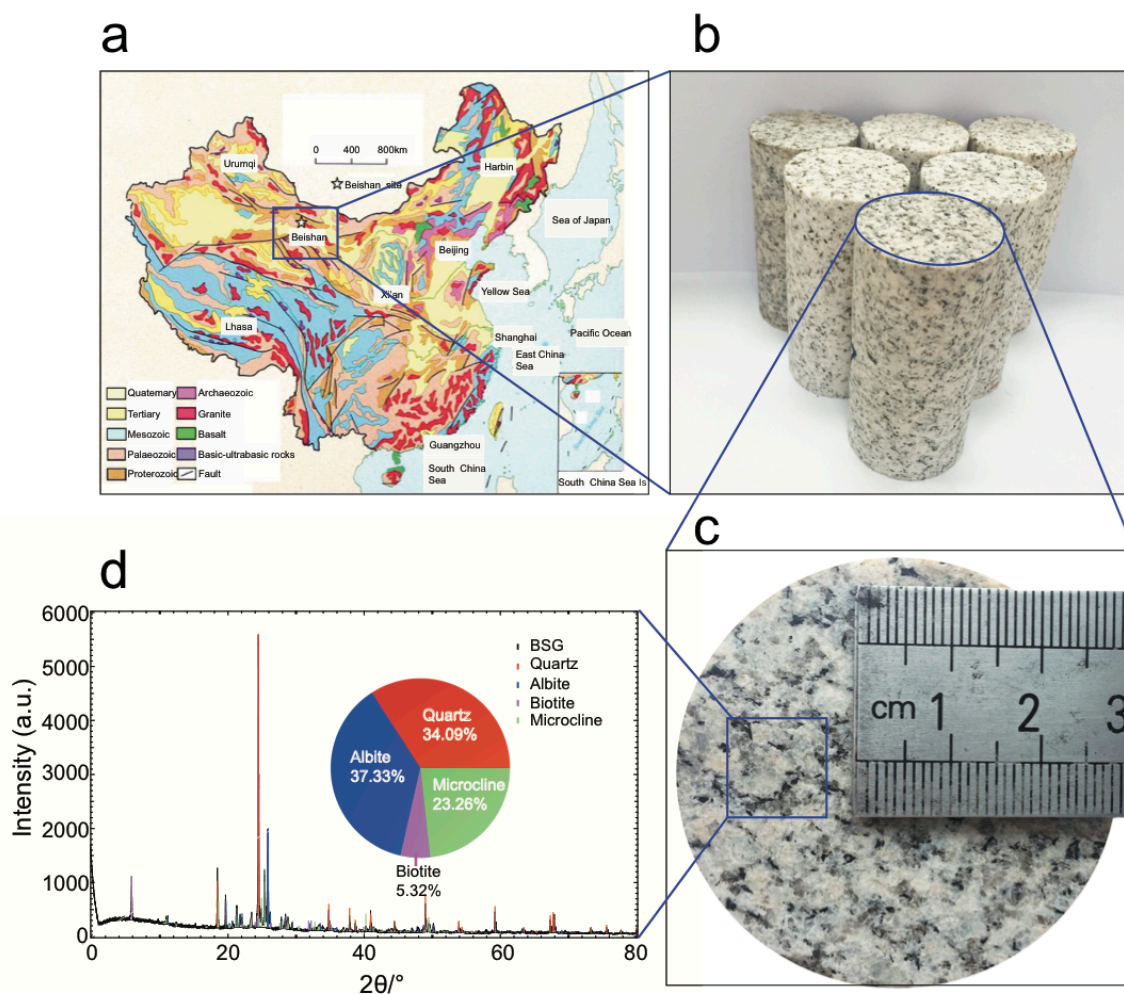
Supplemental Figure S1. (a) Preselected areas for China's high-level radioactive waste repository. Beishan in the northwest of China is marked by a star. (b) The shapes of all BsG specimens are cylinders with 100 mm length and 50 mm diameter. (c) The ends of the samples were smooth within ±0.02mm. (d) The main mineral components.
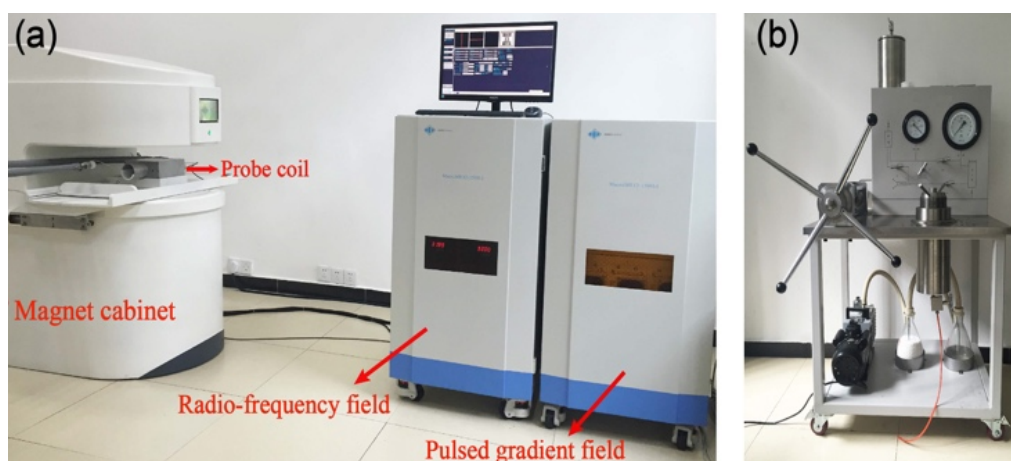
Supplemental Figure S2. (a) Low-field NMR test system, and (b) high-pressure device to inject water into the samples.
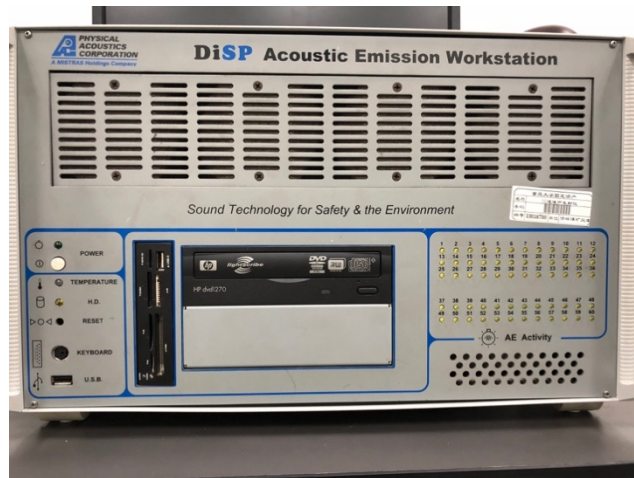
Supplemental Figure S3. DISP acoustic emission workstation from the Physical

Acoustics Company, USA.
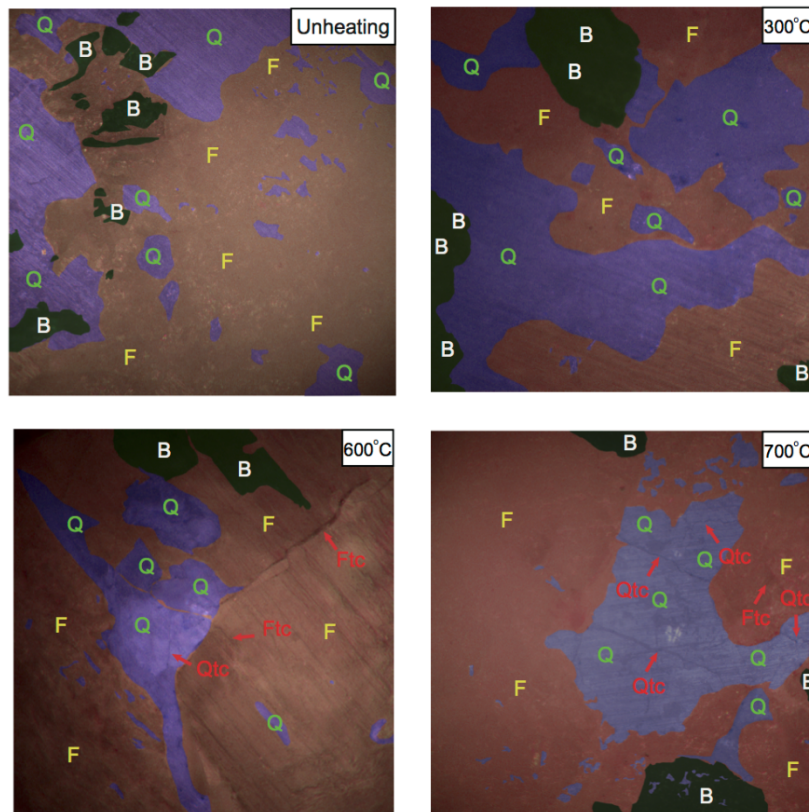
Supplemental Figure S4. Optical microscopic observation of granite specimens for unheating and different anneal temperatures, Q (quartz), F (feldspar), B (biotite), and tc (transgranular cracks)